

## Resonantly enhanced, three-photon ionization of Xe: Optically pumped rare-gas laser

A. W. McCown, M. N. Ediger, and J. G. Eden

*Department of Electrical Engineering, University of Illinois, Urbana, Illinois 61801*

(Received 2 July 1982)

Three-photon ionization of xenon, resonantly enhanced by the Xe  $6p[1/2]_0$  state at  $80\,119\text{ cm}^{-1}$ , is observed when a xenon atom simultaneously absorbs one ArF ( $51\,733\text{-cm}^{-1}$ ) and two XeF ( $28\,482\text{-cm}^{-1}$ ) photons. For ArF and XeF laser intensities in the  $1\text{--}100\text{-MW cm}^{-2}$  range, the peak electron density is more than an order-of-magnitude larger than that obtainable by the nonresonant, two-photon ionization of Xe by ArF. The spontaneous radiative lifetime of the  $6p[1/2]_0$  level and the rate constant for quenching of the state by background Xe atoms were measured to be  $29 \pm 4\text{ ns}$  and  $4 \pm 1 \times 10^{-10}\text{ cm}^3\text{ s}^{-1}$ , respectively. Excitation of the  $6p[1/2]_0$  state is both selective and intense and has resulted in lasing on the  $6p[1/2]_0 \rightarrow 6s[3/2]_1$  transition at  $828.0\text{ nm}$ , which represents the first optically pumped rare-gas laser.

While electron beam and discharge excitation are capable of producing large concentrations of atomic ions in the gas phase, neither possesses the state selectivity that is characteristic of laser pumping but instead produces an array of neutral and ionic species. The large ionization potentials of the rare gases, however, have hindered the widespread application of linear optical pumping techniques and so, in recent years, considerable effort has been expended in developing nonlinear, multiphoton excitation and ionization schemes (involving lasers of high peak power) for the rare gases. Nonresonant multiphoton ionization of the rare gases using ruby<sup>1</sup> or an harmonic of Nd:YAG (Ref. 2) and resonantly enhanced ionization, exploiting the tunability of a dye laser,<sup>3-5</sup> have been demonstrated. Due to the small cross sections inherent with nonresonant processes, the former approach requires enormous ( $>10^9\text{--}10^{10}\text{ W cm}^{-2}$ ) intensities to obtain (even for the heavier rare gases) modest ion densities while the latter generally sacrifices laser pulse energy.

These limitations can be circumvented by utilizing the high peak power and photon energy combinations that are obtainable with the use of two or more rare-gas-halide excimer lasers. With this laser family, two photon-allowed excited states from 7 to  $\sim 13\text{ eV}$  can be studied and no more than four photons are required to ionize any of the rare gases.

Although neutral excited states of Xe and Kr have been produced with excimer laser radiation of a single wavelength, photoionization of only Xe has been reported. The coefficient for two-photon ionization of Xe at  $193\text{ nm}$  (ArF) has been calculated<sup>6</sup> and recently measured<sup>7,8</sup> and three-photon resonant, four-photon ionization of Xe at  $351\text{ nm}$  (XeF) has been observed.<sup>9</sup>

The observation of three-photon ionization of Xe (where  $h\nu_1 \neq h\nu_2 = h\nu_3$ ), resonantly enhanced by the  $6p[1/2]_0$  state at  $80\,119\text{ cm}^{-1}$  ( $2p_5$  in Paschen nota-

tion), is reported in this Communication. The simultaneous absorption of one ArF ( $51\,733\text{ cm}^{-1}$ ) and two XeF ( $28\,482\text{ cm}^{-1}$ ) photons by the atom is found, for laser intensities in the  $1\text{--}100\text{ MW cm}^{-2}$  range, to enhance the  $\text{Xe}^+$  ion production rate by at least an order of magnitude over the two ArF photon, nonresonant process. While representing a modest improvement in the ionization rate for Xe, this approach of exploiting a coincidental near resonance between the energy sum of two (or more) excimer laser photons and a multiphoton accessible state is expected to provide a convenient means for significantly improving the peak ion densities that can be produced in the lighter rare gases.

Figure 1 is a partial energy-level diagram of atomic xenon. The Xe  $6p[1/2]_0$  state lies at  $80\,119\text{ cm}^{-1}$ , which is within  $100\text{ cm}^{-1}$  of the combined photon energies of the XeF ( $3.5\text{ eV/photon}$ ) and ArF ( $6.4\text{ eV/photon}$ ) lasers. An additional photon from either laser is sufficient to ionize an atom in this energy level. However, as will be shown later, a second XeF photon is responsible for the ionization of the  $6p[1/2]_0$  state. The nonresonant two-photon ionization of Xe by two ArF photons is also illustrated in Fig. 1.

A partial schematic diagram of the experimental apparatus is shown in Fig. 2. The rectangular ( $\sim 0.5 \times 2.9\text{ cm}$ ) output beams from an ArF and an XeF laser were focused by two cylindrical quartz lenses to a line collinear with the axis of a suprasil quartz tube. Both lasers were operated as free-running oscillators with pulse widths of  $11\text{--}13\text{ ns}$  full width at half maximum (FWHM). The bulk of the XeF energy was contained in the line at  $351.1\text{ nm}$  having a width of  $41\text{ cm}^{-1}$  FWHM, whereas the ArF laser had a linewidth of  $\sim 140\text{ cm}^{-1}$  FWHM. Also, a digital delay generator made it possible to retard the XeF laser with respect to the ArF pulse. Each optical cell contained between 1 and 300 Torr of research

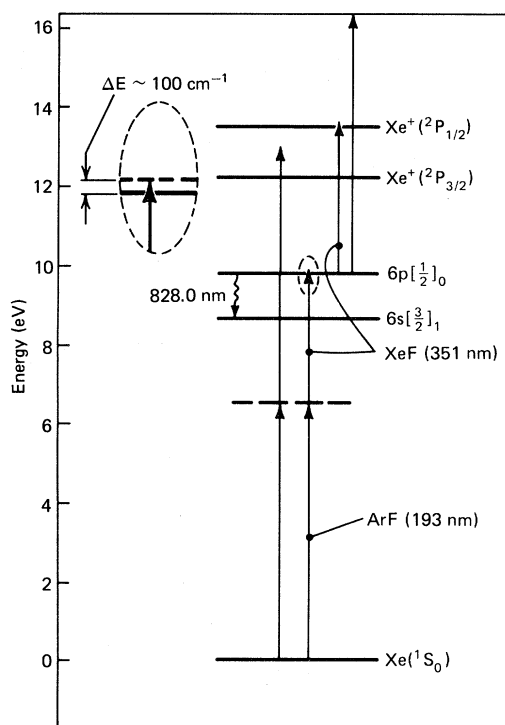


FIG. 1. Partial energy-level diagram for Xe showing two (nonresonant) and three-photon ionization of the atom.

grade Xe and the procedure for cleaning and filling the cells will be described elsewhere.<sup>8</sup>

Temporally resolved measurements of the absolute electron density were carried out by measuring the ac conductivity of the laser-produced plasma. Briefly, the output of a klystron at 9.25 GHz impinged on the optical cell. Due to the presence of the Xe photoelectrons, the microwave signal was both attenuated and shifted in phase. Data acquisition consisted of firing the ArF and XeF lasers, recording the peak intensities of each laser and the photographing transmitted (attenuated) microwave waveform. For a given Xe pressure, XeF and ArF laser intensities, and for  $\nu_m$  (the collision frequency for  $e$ -Xe momentum transfer)  $= 5.0 \times 10^{-9} \text{ cm}^3 \text{ s}^{-1}$  (Ref. 10), the peak electron density was determined from the experimentally measured microwave attenuation. Details of the data analysis, the operation of the microwave system, and the laser intensity measurements can be found in Ref. 8.

The cell was situated in a  $\sim 15$ -cm long section of cylindrical waveguide which had been slotted to permit the entry of the focused laser beams. Fluorescence from the Xe plasma escape through a 6-mm-diam hole drilled in an  $E$  bend in the waveguide and the Xe  $6p[1/2]_0 \rightarrow 6s[3/2]_1$  transition at 828.0 nm was monitored by an RCA C31034A photomultiplier (GaAs photocathode). A dielectric bandpass filter was placed before the photomultiplier to reject ex-

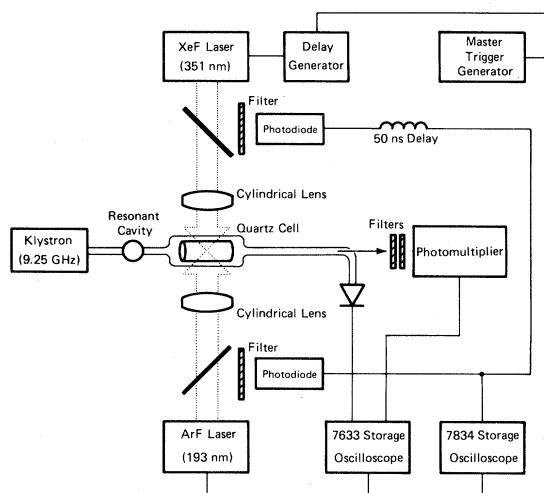


FIG. 2. Schematic diagram of the experimental apparatus. The relative diameters of the cylindrical waveguide and the optical cell have been exaggerated for clarity. Also, the reference arm of the microwave bridge (used to determine  $\nu_m$ ) is not shown.

traneous atomic emission and stray laser radiation.

In most of the previous studies of resonantly enhanced, multiphoton ionization of xenon,<sup>3-5</sup> a dye laser was tuned through an atomic resonance which was readily observable due to a large enhancement in the ion signal. In these experiments, magnification of the ion density was observed as the time delay between the ArF and XeF lasers was varied. The delay between the lasers was determined for each shot from an oscillogram of the pulses and a 50-ns delay line was inserted to avoid overlapping the two laser signals on the oscilloscope display.

The dependence of the electron density on the time delay between the ArF and XeF lasers (XeF fired at  $t=0$ ,  $I_{\text{ArF}}$  and  $I_{\text{XeF}}$  fixed at  $35 \text{ MW cm}^{-2}$  and  $15 \text{ MW cm}^{-2}$ , respectively) is shown in Fig. 3 for a Xe pressure of 100 Torr. As would be expected for a multiphoton process, the data fall symmetrically about  $\Delta t=0$  and the FWHM of the smooth curve is consistent with the pulse widths of the two lasers involved. For  $\Delta t \geq 15 \text{ ns}$ , the bulk of the electron density is due to nonresonant, two-photon ionization of Xe and ArF. The four-photon ionization of Xe at 351 nm, on the other hand, is not detected when XeF is fired alone.

When both lasers irradiate the Xe simultaneously, the peak electron density is found to be  $\sim 15$  times greater than the two ArF photon "background." Since this background varies quadratically with  $I_{\text{ArF}}$ , the enhancement will also be a strong function of  $I_{\text{ArF}}$ . Also, the electron densities in Fig. 3 for  $\Delta t < 6 \text{ ns}$  must be viewed as lower limits inasmuch as the detection limit of the microwave bridge is being approached. The actual values of  $n_e$  are believed to be

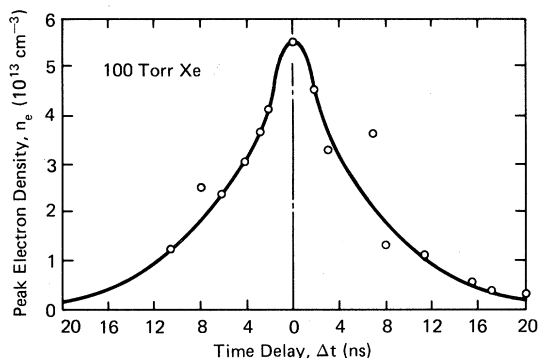


FIG. 3. Variation of the absolute photoelectron density with the time delay between the two lasers. The XeF laser is fired at  $t=0$  and the arrival of the ArF pulse is varied in time as shown.

more than a factor of 2 larger than those indicated.

As a consequence of these results, small laser intensities are required to produce large electron densities (fractional ionizations of  $10^{-3}$ – $10^{-2}\%$ ) and so larger volume plasmas can be produced for a given peak laser power.

The enhancement of the  $\text{Xe}^*$  828.0-nm spontaneous emission was even more dramatic. With ArF firing alone, fluorescence on this transition is observed due to feeding of the  $6p[1/2]_0$  state by dissociative recombination of  $\text{Xe}_2^+$  ions. For  $\Delta t=0$ , however, and ArF and XeF intensities of  $\sim 100 \text{ MW cm}^{-2}$ , the emission on this line rose by over six orders of magnitude due to the selective nature of the pumping process. The peak  $6p[1/2]_0$  population is estimated to be  $10^9$ – $10^{10} \text{ cm}^{-3}$  (for  $p_{\text{Xe}}=100 \text{ Torr}$ ) when indirectly populated by ArF photoionization and rises to  $10^{15}$ – $10^{16} \text{ cm}^{-3}$  for the near-resonant two-photon excitation process.

As shown in Fig. 4, the identity of the third photon in this near-resonant process is indicated by the laser intensity dependence of the peak Xe ion density. In the upper left-hand portion of the graph, the linear variation of  $n_e$  with  $I_{\text{ArF}}$  for  $I_{\text{XeF}}$  fixed at  $16 \text{ MW cm}^{-2}$  is shown. Holding  $I_{\text{ArF}}$  constant, however, and varying the XeF intensity between  $\sim 2$  and  $25 \text{ MW cm}^{-2}$  reveals a near quadratic dependence of the peak

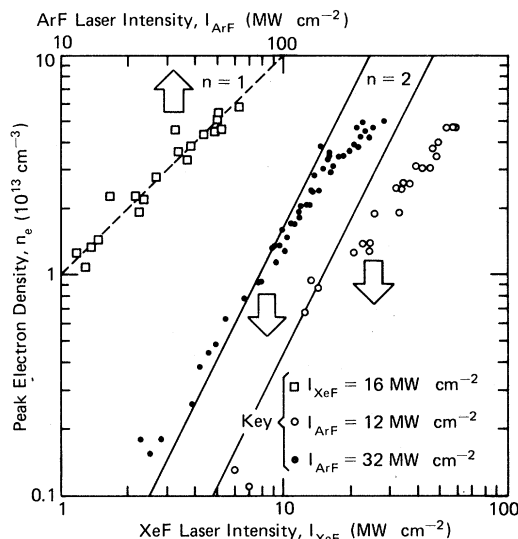


FIG. 4. Dependence of the peak electron density on the ArF and XeF laser intensities. The data show that one ArF and two XeF photons are involved in the ionization process. The Xe pressure is 40 Torr for all of the data shown.

electron density on  $I_{\text{XeF}}$ . The solid lines shown in the figure have a slope of 2 (i.e.,  $n_e \propto I^2$ ) whereas the dashed line has a slope of 1 and thus denotes a linear variation in the electron density. Therefore it appears that a  $\text{Xe}^+$  ( $^2P_{1/2}$ ) ion is produced by the simultaneous absorption of one ArF and two XeF photons. This process is within  $350 \text{ cm}^{-1}$  of being resonant (if line center of both lasers is assumed).

The near-resonant pumping of the Xe ( $6p[1/2]_0$ ) state lends itself to measuring the radiative lifetime and xenon quenching rate constant for the state. Peaking in less than 20 ns, the  $\text{Xe}^*$  fluorescence waveform decays according to a single exponential constant  $\tau$  where

$$\tau^{-1} = \tau_{\text{sp}}^{-1} + k[\text{Xe}] \quad (1)$$

$\tau_{\text{sp}}$  is the spontaneous emission lifetime for the  $6p[1/2]_0$  level and  $k$  is the rate constant for two-body quenching of that state by Xe. Equation (1) is valid when  $\tau$  is at least twice the decay constant for the laser pulse. Thus these measurements were limited

TABLE I. Radiative lifetime  $\tau_{\text{sp}}$  and two-body quenching rate constant  $k$  for the  $\text{Xe}^*6p[1/2]_0$  state.

$\tau_{\text{sp}}$ (ns)	Reference	$k$ ( $\text{cm}^3 \text{ s}^{-1}$ )	Reference
$29 \pm 4$	This work	$(4 \pm 1) \times 10^{-10}$	This work
$40 \pm 12$	Allen <i>et al.</i> <sup>a</sup>		
$30 \pm 4$	Verolainen and Osherovich <sup>b</sup>		
30	Horiguchi <i>et al.</i> <sup>c</sup>		
29.4	Sabbagh and Sadeghi <sup>d</sup>		
25.7	McGuire <sup>e</sup>		

<sup>a</sup>Reference 11.

<sup>b</sup>Reference 12.

<sup>c</sup>Reference 13.

<sup>d</sup>Reference 14.

<sup>e</sup>Reference 15.

to Xe pressures below 3 Torr and the results are summarized in Table I. The  $6p[1/2]_0 \rightarrow 6s[3/2]_1$  transition probability was determined to be  $3.4 \times 10^7 \text{ s}^{-1}$  or  $\tau_{\text{sp}} = 29 \pm 4 \text{ ns}$  (where the branching ratio for the 828.0-nm line is 0.998),<sup>13</sup> which is in excellent agreement with existing experimental and theoretical values. While there is no data in the literature with which the value of  $k$  measured here ( $4 \pm 1 \times 10^{-10} \text{ cm}^3 \text{ s}^{-1}$ ) can be compared, similar rate constants have been reported by Bokor *et al.*<sup>16</sup> for  $6p$  levels in Kr. Also, Horiguchi and co-workers<sup>13</sup> have obtained comparable results ( $k \sim 2\text{--}4 \times 10^{-10} \text{ cm}^3 \text{ s}^{-1}$ ) for the self-quenching of several  $7p$  and  $6p'$  levels in xenon.

The large Xe  $6p$  excitation rates that can be realized with this two-excimer photon ( $h\nu_1 \neq h\nu_2$ ) scheme have also led to the observation of the first optically pumped rare-gas laser.<sup>17</sup> With a single, uncoated quartz flat acting as a low-reflectivity mirror, stimulated emission on the 828.0-nm line was observed for Xe pressures above 20 Torr. The gain length for the laser was  $\sim 3 \text{ cm}$  (the width of each excimer beam). Stimulated emission was observed only for  $\Delta t \leq 4 \text{ ns}$  and with the quartz flat (or a mirror) installed. A typical laser waveform is illustrated in Fig. 5. Onset of lasing occurs  $\sim 8 \text{ ns}$  after the initiation of the XeF pulse (leakage of 351-nm laser radiation through the bandpass filter is shown at the bottom of the figure) at which time the ArF and XeF intensities have peaked. The small ( $\sim 4 \text{ ns}$ ) half width and rapid termination of the laser pulse are simply attributed to the declining excitation rate.

In summary, three-photon ionization of Xe, resonantly enhanced by the Xe  $6p[1/2]_0$  state, has been observed when one ArF and two XeF excimer laser photons ( $h\nu_1 \neq h\nu_2 = h\nu_3$ ) are simultaneously absorbed by a ground-state Xe atom. With this technique, the production of large ( $10^{12}\text{--}10^{15} \text{ cm}^{-3}$ ) ion

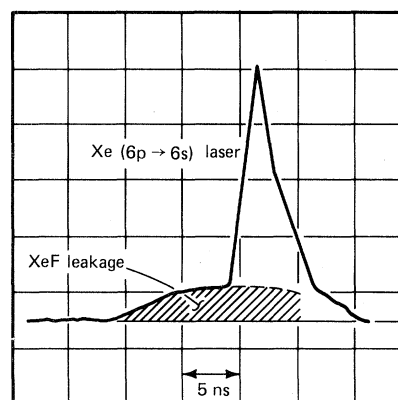


FIG. 5. Representative Xe 828.0-nm laser waveform that is observed when 20-Torr Xe is irradiated simultaneously by ArF and XeF pulses. The leakage of XeF radiation through the bandpass filter is also indicated.

and excited-state populations with moderate ( $\leq 10^8 \text{ W cm}^{-2}$ ) laser intensities is within reach for the lighter rare gases as well. Considering only the use of the rare-gas-fluoride lasers, two-photon resonant, three-photon ionization of Kr and an analogous four-photon ionization process in Ar are possible and involve detunings of  $< 50 \text{ cm}^{-1}$  (for free-running oscillators). Such schemes will undoubtedly provide a new tool for the study of rare-gas ion chemistry and recombination.

The authors extend their thanks to J. T. Verdeyen for many excellent suggestions with regard to the microwave measurements and to K. Kuehl, Y. Moroz, and A. B. Wilson for excellent technical assistance. The support of this work by the NSF (R. E. Rostenbach) under Grant No. CPE 80-06378 is gratefully acknowledged.

<sup>1</sup>G. S. Voronov and N. B. Delone, Zh. Eksp. Teor. Fiz. **50**, 78 (1966) [Sov. Phys. JETP **23**, 54 (1966)].

<sup>2</sup>L. A. Lompre, G. Mainfray, G. Manus, and J. Thebault, Phys. Rev. A **15**, 1604 (1977).

<sup>3</sup>K. Aron and P. M. Johnson, J. Chem. Phys. **67**, 5099 (1977).

<sup>4</sup>C. H. Chen, G. S. Hurst, and M. G. Payne, Chem. Phys. Lett. **75**, 473 (1980).

<sup>5</sup>R. N. Compton, J. C. Miller, A. E. Carter, and P. Kruit, Chem. Phys. Lett. **71**, 87 (1980); J. C. Miller and R. N. Compton, Phys. Rev. A **25**, 2056 (1982); J. C. Miller, R. N. Compton, M. G. Payne, and W. W. Garrett, Phys. Rev. Lett. **45**, 114 (1980).

<sup>6</sup>W. K. Bischel, J. Bokor, D. J. Klinger, and C. K. Rhodes, IEEE J. Quantum Electron. **QE-15**, 380 (1979).

<sup>7</sup>R. V. Hodges, L. C. Lee, and J. T. Moseley, Int. J. Mass Spectrom. Ion Phys. **39**, 133 (1981).

<sup>8</sup>A. W. McCown, M. N. Ediger, and J. G. Eden, Phys. Rev. A (in press).

<sup>9</sup>M. Rothschild, J. Zavelovich, W. Gornik, and C. K. Rhodes, Opt. Commun. **39**, 316 (1981).

<sup>10</sup>Using the complete microwave bridge described in Ref. 8,  $\nu_m$  was measured for XeF and ArF simultaneously impinging on the optical cell.

<sup>11</sup>L. Allen, D. G. C. Jones, and D. G. Schofield, J. Opt. Soc. Am. **59**, 842 (1969).

<sup>12</sup>Y. F. Verolainen and A. L. Osherovich, Opt. Spektrosk. **27**, 31 (1969) [Opt. Spectrosc. **27**, 14 (1969)].

<sup>13</sup>H. Horiguchi, R. S. F. Chang, and D. W. Setser, J. Chem. Phys. **75**, 1207 (1981).

<sup>14</sup>J. Sabbagh and N. Sadeghi, J. Quant. Spectrosc. Radiat. Transfer **17**, 297 (1977).

<sup>15</sup>E. J. McGuire, Phys. Rev. A **24**, 835 (1981).

<sup>16</sup>J. Bokor, J. Y. Zavelovich, and C. K. Rhodes, Phys. Rev. A **21**, 1453 (1980).

<sup>17</sup>Silfvast and co-workers [W. T. Silfvast, L. H. Szeto, and O. R. Wood II, Appl. Phys. Lett. **31**, 334 (1977)] have report lasing from Ar, Kr, and Xe in a CO<sub>2</sub> laser-produced plasma but the pumping mechanism is recombination rather than optical excitation.